

# Carrier-induced formation of electrically active boron-interstitial clusters in irradiated boron-doped silicon

Cite as: J. Appl. Phys. 135, 055101 (2024); doi: 10.1063/5.0172704

Submitted: 21 August 2023 · Accepted: 15 January 2024 ·

Published Online: 1 February 2024



X. C. Chen,<sup>1,a)</sup> L. Li,<sup>1</sup> M. Y. Wang,<sup>2</sup> H. Ren,<sup>3</sup> X. Q. Liu,<sup>1</sup> G. Zeng,<sup>1</sup> and G. X. Yang<sup>1</sup>

## AFFILIATIONS

<sup>1</sup>Institute of Nuclear Physics and Chemistry, China Academy of Engineering Physics, Mianyang 621900, China

<sup>2</sup>State Grid Nanchong Electric Power Supply Company, Nanchong 637000, China

<sup>3</sup>School of Materials Science and Engineering, China University of Petroleum (East China), Qingdao 266580, China

<sup>a)</sup>Author to whom correspondence should be addressed: [xcchen@caep.cn](mailto:xcchen@caep.cn)

## ABSTRACT

Excess minority carriers create boron-related recombination centers that degrade the efficiency of the non-particle-irradiated silicon solar cells. However, the carrier-induced reactions among the radiation-induced defects are poorly understood for devices exposed to particle radiation. This study investigates the structure, electronic properties, formation and annihilation mechanisms, and diffusion dynamics of the carrier-induced defects in particle-irradiated boron-doped silicon using density-functional modeling and junction spectroscopy. By revisiting the ground-state structures of the boron-di-interstitial clusters ( $BI_2$ ), we find that the calculated acceptor and donor levels of such defects agree well quantitatively with the carrier-induced deep-level transient spectroscopy (DLTS) hole emission signatures at 0.43 and 0.53 eV above the valence band edge ( $E_v$ ), respectively. We also find that the formation of  $BI_2$  is thermally activated by an energy of 0.50 eV, which we explain theoretically by the reduction of the migration barrier of mono-interstitials to 0.53 eV in the presence of excess minority carriers. Moreover, we discover that the  $BI_2$  are potentially mobile with a migration barrier of 1.18 eV, contrary to the present understanding.

Published under an exclusive license by AIP Publishing. <https://doi.org/10.1063/5.0172704>

## I. INTRODUCTION

Carrier-induced defect formation and transformation have detrimental effects for boron-doped silicon semiconductor devices. A continuous interest has been devoted to such effects occurring in the silicon solar cells for almost 50 years (also known as light-induced degradation, e.g., Ref. 1), where the formation of electrically active boron-oxygen complexes, via either above-bandgap illumination or forward biasing, has been considered to result in a significant drop in the carrier lifetime and, hence, the cell efficiency. While most of the previous works have been focused on such carrier-induced phenomena occurring only in the non-particle-irradiated solar cells, however, the carrier-induced reactions and transformations among the radiation-induced defects remain much more elusive for boron-doped silicon devices exposed to intense particle radiation such as in outer space. Without careful scrutiny of such carrier-induced processes, it is not possible to predict the reliability of the electronics in the radiation environment over their lifespan.

Such issues have been raised more recently regarding the carrier-induced changes of electrical properties of the particle-irradiated devices, such as the effect doping concentration of the bulk devices, the leakage current and the charge collection efficiency of the radiation detectors,<sup>2–5</sup> and the current gain of the bipolar transistors.<sup>6–8</sup> One of the major concerns is the creation of a considerable amount of defect centers at 0.43 and 0.53 eV above the valence band edge ( $E_v$ ), respectively, by the injection of excess carriers in the B-doped silicon after exposure to particle irradiation; this has been reported to significantly degrade the electrical performance of the silicon bipolar devices.<sup>8–10</sup> However, the knowledge regarding the composition and dynamics of such defect centers is far from clear. These defect centers were initially assigned to carbon-di-interstitial complexes ( $CI_2$ ),<sup>11</sup> and later by re-examining the concentrations of the impurity atoms, the defect assignment was then revised to boron-di-interstitial clusters ( $BI_2$ ).<sup>10</sup> In the previously proposed models,<sup>9–11</sup>  $BI_2$  are considered to be formed due to the trapping of a mobile di-interstitial by boron, which are

03 February 2024 06:47:33

released by di-interstitial-oxygen complexes ( $I_2O$ ), and can transform between two configurations via the reversible injection-annealing cycles. However, further experiments<sup>8</sup> challenge these models by showing the increase in the effective doping concentrations upon defect formation, whereas the decrease in the effective dopants is expected according to the models in Refs. 9–11.

In this study, we identify new ground-state structures for  $BI_2$  and confirm the assignment of the  $E_v+0.43$  eV and  $E_v+0.53$  eV defect centers to  $BI_2$  by reproducing the electronic and dynamical properties with *ab initio* calculations. Neither the formation of  $BI_2$  involving  $I_2O$  breakup nor the configurational transformations of  $BI_2$  upon carrier injection proposed in the previous models are supported by our further experimental evidence. We instead propose the charge-state-dependent migration behavior of the mono-interstitials ( $I$ ) to be attributed to the carrier-induced formation of the deep recombination centers  $BI_2$ . Such a process of defect formation may also be responsible for the carrier-induced degradation in the non-particle-irradiated silicon. We also indicate that the mobility of  $BI_2$  should be considered contrary to the assumptions of most defect models;<sup>12–17</sup> it can diffuse by a two-step process consisting of translation and reorientation with a barrier of 1.18 eV.

## II. METHOD DETAILS

### A. Calculation details

*Ab initio* calculations were carried out with a plane-wave density-functional code, CASTEP.<sup>18</sup> For each system, the generalized gradient approximation (GGA) ultrasoft pseudopotential<sup>19,20</sup> was employed for the search of the ground-state and saddle point structures along the minimum energy paths of atomic mechanisms, and then the hybrid density functional of Heyd-Scuseria-Ernzerhof (HSE06)<sup>21,22</sup> with a norm-conserving pseudopotential was performed for the single-point energy calculations. This two-step method, first calculating a GGA-level structure followed by a single-point energy calculation within HSE06, has been shown to be quite accurate in terms of formation energies and migration barriers.<sup>23,24</sup> 216-atom supercells of silicon were used, in which self-interstitials and boron atoms were inserted to produce defects. The Brillouin zone of GGA- and HSE06-level calculations was sampled at  $2 \times 2 \times 2$  and  $1 \times 1 \times 1$   $k$ -point meshes, respectively. The nudged elastic band method<sup>25</sup> was adopted to investigate defect migration and transformation. The energy cutoff was 400 eV. Atoms were relaxed until the forces were less than 0.03 eV/Å.

The stability of the defects was calculated through the use of formation energies. The formation energy ( $E_f^Q$ ) of defects with the charge state  $Q$  is evaluated as<sup>26</sup>

$$E_f^Q = (E_D^Q - E_X^0) + Q(\varepsilon_F + \varepsilon_v) - \sum_s n_s \mu_s + E_{\text{corr}}, \quad (1)$$

where  $E_D^Q$  is the calculated total energy of the supercell containing the defect  $D$ ,  $E_X^0$  is the total energy of the corresponding perfect crystal supercell,  $\varepsilon_F$  is the Fermi level,  $\varepsilon_v$  is the top of the valence band,  $n_s$  is the number of atoms of species  $s$ ,  $\mu_s$  is the chemical potential corresponding to that species, which is not critical since the quantities of interest (the total-energy differences and the

ionization levels of defects) do not depend on the chemical potentials, provided that the defects compared contain the same number of Si and B atoms, and  $E_{\text{corr}}$  is the correction term accounting for any spurious effects such as the finite-size supercell errors. Unfortunately,  $E_{\text{corr}}$  is sensitive to the defect species and their respective charge states and is practically hard to obtain.<sup>27</sup> We employed the *marker method* to cancel out the  $E_{\text{corr}}$  term by introducing appropriate experimental data. This method basically assumes that the offsets of the ionization potentials between the calculated defect and the marker defect that is well established experimentally are essentially identical to that of the calculated defect level and the experimentally observed marker level.<sup>28,29</sup> Although the formation energy method with the supercell-size corrections, e.g., Ref. 30, has become popular in the last 10 years, the empirical marker method has proved to be an efficient way to cancel the systematic errors derived from the non-exact treatment of the electronic exchange-correlation and finite-size effects.<sup>31</sup> The formation energy method and the marker method are reported to be essentially equivalent<sup>32</sup> and agree to within 0.1 eV.<sup>33,34</sup> The application of this method has successfully reproduced many defect levels in semiconductor including silicon,<sup>34–43</sup> diamond,<sup>44</sup> and 2D materials.<sup>45–47</sup>

By comparing the total energy differences between the relaxed, positively (negatively) charged states, and the neutral defects,  $\Delta E(Q/Q+1) \equiv E_D^Q - E_D^{Q+1}$ , for the defect under scrutiny (subscripted with “d”) with that of a marker defect (subscripted with “m”), the calculated defect level  $E_d(Q/Q+1)$  is predicted at<sup>28,29</sup>

$$E_d(Q/Q+1) \approx E_m(Q/Q+1) + \Delta E_d(Q/Q+1) - \Delta E_m(Q/Q+1), \quad (2)$$

where  $E_m(Q/Q+1)$  is the experimentally observed level of the marker defect. The formation energies of the charged defects relative to their neutral states are, hence, expressed as

$$E_f^{+1} - E_f^0 = \varepsilon_F - [\Delta E_d(Q/Q+1) - \Delta E_m(Q/Q+1) + E_m(Q/Q+1)], \quad (3a)$$

$$E_f^{-1} - E_f^0 = -\varepsilon_F + [\Delta E_d(Q/Q+1) - \Delta E_m(Q/Q+1) + E_m(Q/Q+1)], \quad (3b)$$

where  $E_X$ ,  $\varepsilon_v$ , and  $\sum_s n_s \mu_s$  in Eq. (1) all cancel out. The error of the marker method is eliminated when the marker defect has ideally similar electronic properties to the defect under scrutiny. We selected the interstitial boron (BI) as the marker with the well-known donor and acceptor levels as listed in Table SI in the [supplementary material](#).

### B. Experiment details

The samples studied here were a group of  $p$ - $n$ - $p$  silicon bipolar devices made by growing an epitaxial  $p$ -type silicon layer that is subsequently phosphorus and boron doped which the doping profiles by secondary-ion-mass spectroscopy (SIMS) have

been previously described in detail elsewhere.<sup>8,48,49</sup> The defects were introduced at room temperature by 14 MeV fusion neutron irradiation (by bombarding the deuterium target with triton beams) to fluences of  $10^{13} \text{ cm}^{-2}$ . All leads were shorted during both the irradiation and annealing treatments. The minority carriers were injected into the base/collector diode with the emitter shorted to the base. All the injection and annealing treatments were performed in the vacuum chamber of the junction spectroscopy apparatus. The experimental results in the present work were obtained by means of deep-level transient spectroscopy (DLTS) and minority-carrier transient spectroscopy (MCTS). Both majority (DLTS) and minority (MCTS) carrier spectra were recorded with a rate window of  $255.8 \text{ s}^{-1}$ , filling pulse width of 100 ms, and bias of  $-9.5 \text{ V}$ , while the filling pulse amplitude was set to 9.5 and 10.5 V for the majority and minority-carrier measurements, respectively. The DLTS/MCTS spectra were acquired using the base/collector diode with the emitter shorted to the base.

### III. RESULTS

#### A. Electronic properties

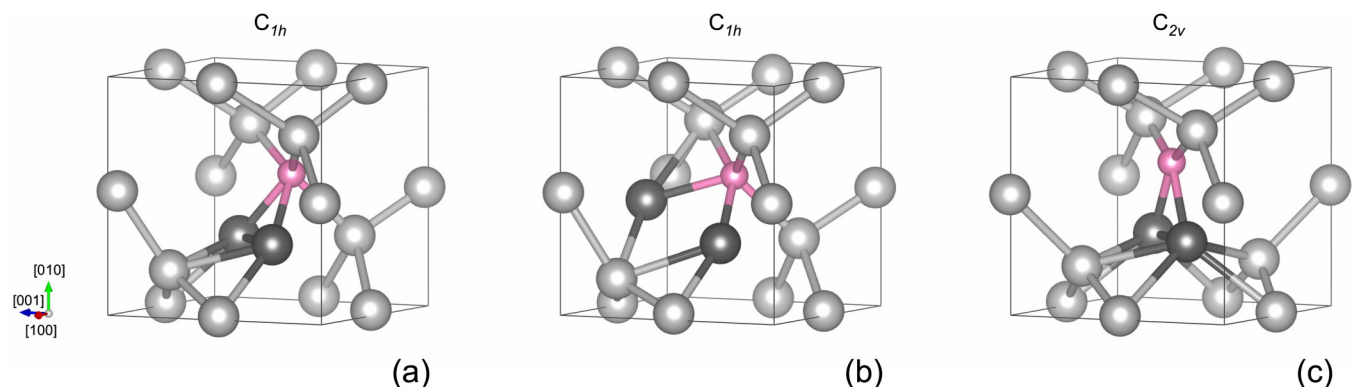
Our calculations identified three  $\text{BI}_2$  states labeled  $\text{BI}_2^a$ ,  $\text{BI}_2^b$ , and  $\text{BI}_2^c$  as shown in Fig. 1. The  $\text{BI}_2^a$  has  $C_{1h}$  symmetry, which resembles the ground-state structure of di-interstitial ( $\text{I}_2$ )<sup>50–52</sup> except that a boron atom replaces the central interstitial Si atom. Previous studies have reported this structure.<sup>53–57</sup> The  $\text{BI}_2^b$  also has  $C_{1h}$  symmetry and forms a planar configuration, where the two interstitial silicon atoms and the boron atom all lie in the (110) plane. The  $\text{BI}_2^c$  has  $C_{2v}$  symmetry with the clustered interstitial silicon and boron atoms lying in the (101) plane. As discussed later, the  $\text{BI}_2^b$  corresponds to one local minimum configuration after rotation in the two-step diffusion pathway, and the  $\text{BI}_2^c$  corresponds to the other local minimum configuration by a subsequent translation of  $\text{BI}_2^b$  within the (110) plane. Previous studies considered  $\text{BI}_2^a$  as the ground state in  $p$ -type silicon ( $\text{BI}_2^+$ ),<sup>53–57</sup> but we found that it to be metastable by 0.20 eV (0.14 eV) in the 1+ charge state with the HSE (PBE) functional (see Table SII in the

supplementary material). The ground-state structures depend on the functionals; PBE favors  $\text{BI}_2^b$  while HSE prefers  $\text{BI}_2^c$ . However, the energy differences between  $\text{BI}_2^b$  and  $\text{BI}_2^c$  are small: 0.03 eV (0.06 eV) with HSE (PBE).

Figure 2 shows the formation energies and the charge-transfer levels of  $\text{BI}_2$  calculated by HSE06. The charge-transfer levels  $\epsilon(-/0)$  and  $\epsilon(0/+)$  at  $E_v + 0.47 \text{ eV}$  and  $E_v + 0.54 \text{ eV}$ , respectively, match well with the single electron emission signatures  $H(228\text{K})$  and  $H(256\text{K})$  measured by DLTS at  $E_v + 0.43 \text{ eV}$  and  $E_v + 0.53 \text{ eV}$ , respectively.<sup>8–10</sup> The lower position of  $\epsilon(-/0)$  than  $\epsilon(0/+)$  implies a negative- $U$  behavior for  $\text{BI}_2$ . We note that transitions measured by optical absorption and luminescence should differ from the levels demonstrated in Fig. 2. A Franck-Condon shift of 0.23 eV (by HSE) is calculated for the photon-excited process of  $\text{BI}_2^+$ . This Franck-Condon effect is illustrated by the configuration-coordinate total energy diagram in Fig. S1 in the supplementary material. Based on previous theoretical<sup>56</sup> and experimental<sup>8</sup> studies, charge states above 1+ and below 1– are unstable in the bandgap and, thus, are not considered in this paper.

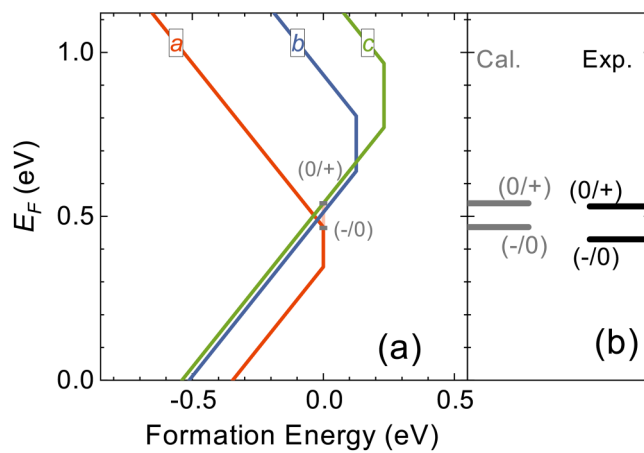
#### B. Dynamic properties

Figure 3(a) shows the minority-carrier transient spectroscopy (MCTS) measurements of the boron-doped silicon subjected to the same reversible cycles of annealing and injection as in Ref. 8. Despite the agreement on the growth of the  $H(228\text{K})$  and  $H(256\text{K})$  peaks upon minority carrier injection, we note that neither the hole emission signature in the range of 50–70 K (assigned to  $\text{I}_2\text{O}^{10,11}$ ) nor the electron emission signature in the range of 160–180 K (labeled ME1 and assigned to one configuration of  $\text{BI}_2^{10}$ ) was observed in our samples. In their previously proposed model,<sup>10,11</sup>  $\text{BI}_2$  form when the mobile di-interstitial ( $\text{I}_2$ ) released by the breakup of  $\text{I}_2\text{O}$  is trapped at a substitutional boron, and the configurational transformation of  $\text{BI}_2$  is indicated by the correlated changes of  $H(228\text{K})/H(256\text{K})$  and ME1 peaks via injection-annealing cycles. It is noted that  $H(228\text{K})/H(256\text{K})$  can be formed at a temperature as low as 250 K as shown in Fig. 3(b), which is far lower than the dissociation temperature of  $\text{I}_2\text{O}$  starting



**FIG. 1.** Calculated atomic structures of  $\text{BI}_2$  in three possible configurations. Magenta balls denote boron atoms, and darker gray balls denote interstitial silicon atoms. (a)  $\text{BI}_2^a$ , (b)  $\text{BI}_2^b$ , and (c)  $\text{BI}_2^c$  configuration.

03 February 2024 06:47:33



**FIG. 2.** (a) Formation energies for  $BI_2$  as a function of the Fermi level ( $E_F$ ) and (b) the corresponding electrical level diagram. The red, blue, and green lines represent the configurations of  $BI_2^a$ ,  $BI_2^b$ , and  $BI_2^c$ , respectively. The light-colored lines show the energetically unfavorable charge states. The energies of the charge-neutral  $BI_2^a$  configurations are set to zero. The  $\epsilon(-/0)$  and  $\epsilon(0/+)$  levels marked by gray horizontal lines correspond to the  $H(228\text{ K})$  and  $H(256\text{ K})$  traps detected by DLTS.

at 330 K.<sup>9,10</sup> Hence, it is concluded that  $I_2O$  plays little or no role in the formation of  $BI_2$ . By extracting the fitted reaction rate constant, Fig. 3(b) shows the Arrhenius behaviors for both generation and annihilation processes of the defect centers, and the activation energies are determined to be 0.50 and 0.93 eV, respectively. The pre-exponential factor of  $\sim 10^5$  determined from carrier injection further reflects a long-range migration character rather than a single jump or reorientation upon defect formation.

Considering the experimental evidence above, we attribute the carrier-induced defect formation of  $BI_2$  to the charge-state-dependent diffusion of the reactant species, the silicon mono-interstitials ( $I$ ). Although  $I$  has a tendency to aggregate to large interstitial clusters  $I_n(n > 3)$ ,<sup>58–60</sup> a larger amount of mono-interstitials are found to survive from clustering in the post-irradiation silicon.<sup>16,17,61</sup> Previous density functional calculations using a GGA functional,<sup>52,56,62,63</sup> a hybrid functional,<sup>64</sup> a GW scheme,<sup>65</sup> or an H-terminated cluster method<sup>66,67</sup> have all made an agreement that the +2 charge state ( $I^{2+}$ ) is predominant when the Fermi level is located at the lower half of the bandgap. For  $p$ -type silicon, the stable charge state  $I^{2+}$  is almost immobile with a migration barrier of 1.49 eV (by HSE). By injecting minority carriers,  $I^{2+}$  is able to trap an electron, becoming  $I^+$ , and  $BI_2$  can form by capturing two mobile  $I^+$  at a substitutional boron site with the migration barrier greatly reduced from 1.49 to 0.53 eV (by HSE). We plot the configuration-coordinate diagram for both the +2 and the +1 charged  $I$  (by PBE) in Fig. S2 in the [supplementary material](#). It is noteworthy that previous studies have reported the overestimation of HSE on the defect migration barrier.<sup>68</sup> However, as listed in Table I, the discrepancies are small between the barriers obtained using HSE and PBE.

The diffusion pathway for  $BI_2$  is demonstrated in Fig. 4. This trajectory consists of a rotation and then a translation step with

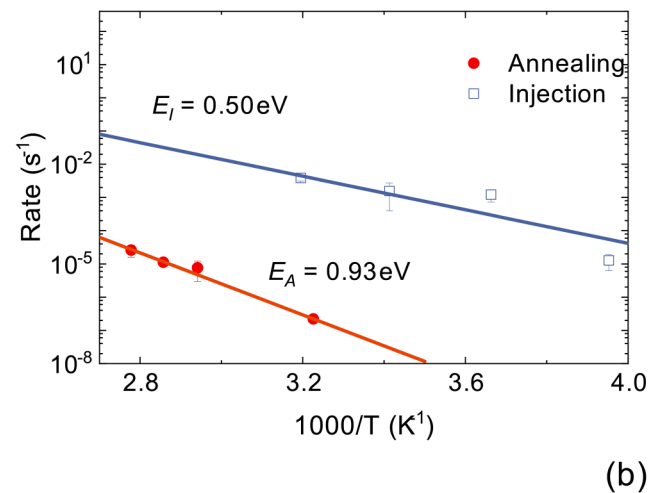
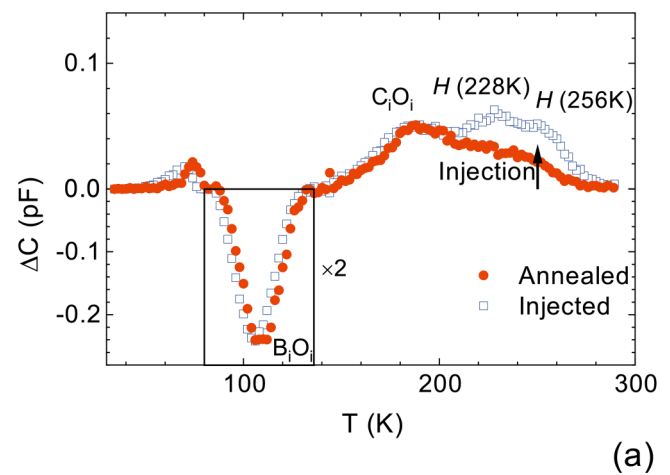


**FIG. 3.** (a) MCTS spectra of the base-collector diode of fusion neutron damaged  $p$ - $n$ - $p$  transistors. The open symbols are obtained immediately after annealing for 2 h at 350 K. The solid symbols are obtained subsequently after forward current injection with density of  $12.5\text{ A} \cdot \text{cm}^{-2}$  at 293 K for 20 min. (b) Arrhenius plot for the formation and annealing rates of the  $H(228\text{ K})$  and  $H(256\text{ K})$  traps obtained by DLTS. The growth of these two traps is measured upon  $2.5\text{ A} \cdot \text{cm}^{-2}$  forward current injection.

similarities to  $I_2$  and  $AsI_2$ .<sup>69,70</sup> The interstitial silicon atom (2) in the ground-state configuration  $BI_2^c$  is initially rotated by  $60^\circ$  about the  $[11\bar{1}]$  axis, with the clustered atoms lying in the  $(101)$  plane changing to the  $(1\bar{1}0)$  plane in order to reach the  $BI_2^b$  configuration. With all the subsequent translational movements constrained in the  $(1\bar{1}0)$  plane, the clustered atoms are then translated to the nearby  $BI_2^c$  site by kicking out the atom (1) to form the interstitial pair and relaxing the atom (3) back to the lattice site. The rotation from  $BI_2^c$  to  $BI_2^b$  has a barrier of 0.50 eV, and the translation to the neighboring  $BI_2^c$  site has a barrier of 1.18 eV. Such relatively low migration barrier for the  $BI_2$  is against

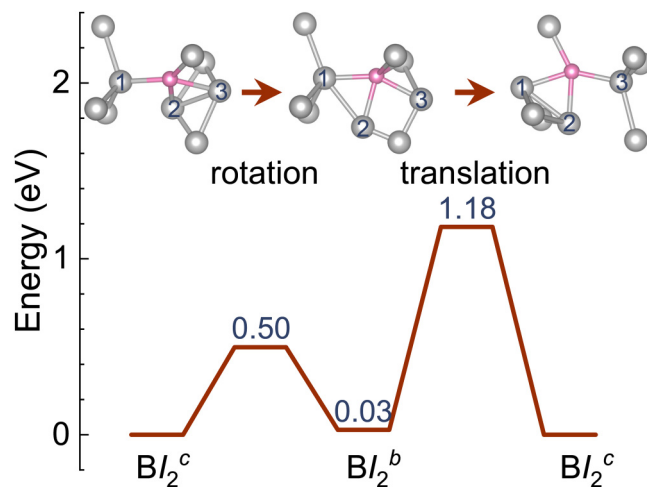
03 February 2024 06:47:33

**TABLE I.** Migration barriers of  $I^{2+}$ ,  $I^+$ , and  $BI_2^+$ . The results from PBE and HSE06 are compared. All values are reported in eV.

	PBE	HSE06
$I^{2+}$	0.55	0.53
$I^+$	1.33	1.49
$BI_2^+$	1.24	1.18

the present understanding of processes such as boron transient enhanced diffusion (TED), where this cluster has been considered to be immobile and act as precursors for the growth of larger boron-interstitial clusters.<sup>12,13</sup> Due to its migration barrier of 1.18 eV,  $BI_2$  may diffuse away and interact with other defects far below the TED temperature of  $\sim 800^\circ\text{C}$ . The mobility of  $BI_2$  should be included in the continuum models regarding the defect annealing process.

Dissociation energies for  $BI_2$  were reported in Ref. 15 via the  $B_s + I_2$  reaction ranging from 1.10 to 1.77 eV and via the  $BI + I$  reaction ranging from 2.60 to 2.99 eV with the assumption that all defect species are neutral. By considering the  $\epsilon(2+/0)$  level at  $E_v + 0.2$  eV for  $I_2$ ,<sup>52</sup> the  $\epsilon(+/0)$  level at  $E_v + 0.53$  eV for  $BI_2$ , and the  $\epsilon(0/-)$  level at  $E_v + 0.05$  eV for  $B_s$ , the dissociation energy for the favored reaction path  $B_s + I_2$  is modified to range from 1.02 to 1.69 eV. However, it should be noted that those values may be underestimated since further EPR experiments have indicated a larger value of 0.88 eV for  $I_2$  in *p*-type silicon<sup>71</sup> rather than the significantly smaller value of 0.26 eV adopted in Ref. 15. Therefore,  $BI_2$  are unlikely to dissociate before diffusing away.

**FIG. 4.** The diffusion pathway of positively charged  $BI_2$ . The path consists of a combination of two steps, rotation and translation. The rotation from  $BI_2^c$  to  $BI_2^b$  has a barrier of 0.50 eV, and the translation to the neighboring  $BI_2^c$  site has a barrier of 1.18 eV. Magenta balls denote boron atoms, and gray balls denote silicon atoms. The moving silicon atoms are marked with numbers. Shown is the (110) projection of the  $BI_2$ .**TABLE II.** The energy levels of  $BI_2$  and the activation energies for formation and annealing obtained from DLTS measurements as well as *ab initio* calculations. All values are in eV.

	Exp.	Cal.
$\epsilon(0/+)$	$E_v + 0.53$	$E_v + 0.54$
$\epsilon(-/0)$	$E_v + 0.43$	$E_v + 0.47$
$E_{\text{form}}$	0.50	0.53
$E_{\text{ann}}$	0.93	0.95 <sup>72</sup>

#### IV. DISCUSSIONS

Table II lists the electronic levels and reaction dynamics of the carrier-induced centers determined by junction spectroscopy and reproduced by the  $BI_2$  defect models with *ab initio* calculations. A generally very good agreement between experiments and calculations supports the assignment of the DLTS signals to the energy levels of  $BI_2$  and the carrier-induced formation mechanisms proposed by us. Although the experimental activation energy of 0.93 eV for the defect annealing is lower than the calculated migration barrier of 1.18 eV for the  $BI_2$ , this discrepancy indicates that faster annihilation channels may exist in the irradiated B-doped silicon before the  $BI_2$  migrate to sinks. For example,  $BI_2$  may capture a mobile  $BI$  to form a larger cluster<sup>13</sup> with a migration barrier of 0.95 eV for  $BI^+$  to overcome<sup>72</sup> assumed from the evidence of plenty of boron and interstitial atoms supplied in the samples. Our present model can also explain the experimental findings that acceptors in the lower half of the bandgap are produced upon minority carrier injection,<sup>8</sup> where two minority carriers are consumed by the reaction of cluster formation, i.e.,  $B^- + 2I^{2+} + 2e^- \rightarrow BI_2^+$ . These experimental data can rule out the acceptor removal model of  $B_s^- + I_2O \rightarrow BI_2^+ + O_i + 2e^-$  in Refs. 10 and 11 in terms of the changes of the effective doping concentrations.

For non-particle-irradiated boron-doped silicon, it has been proposed that the carrier-induced formation of recombination centers responsible for the solar cell degradation is associated with the charge-state-driven diffusion of the oxygen dimers ( $O_{2i}$ ).<sup>73–76</sup> However, further experimental data have cast doubt on the  $B_sO_{2i}$  formation process due to the lack of evidence for the existence of the doubly positively charged oxygen dimer ( $O_{2i}^{++}$ ).<sup>77</sup> Due to the similarities of the reversible injection-annealing cycles and the thermal activation energies in both particle-irradiated and non-particle-irradiated boron-doped silicon (the annihilation and recovery activation energies of  $\sim 1.0$  and  $\sim 0.4$  eV, respectively, in non-particle-irradiated silicon as summarized in Ref. 78), it is natural to link the role of the mono-interstitials to the formation of recombination centers in non-particle-irradiated solar cells. With a much lower concentration of interstitials in non-particle-irradiated silicon, more precise experiments are needed.

#### V. CONCLUSION

In summary, we have studied the structure, electronic properties, formation and annihilation mechanisms, and diffusion dynamics of the  $BI_2^+$  clusters in particle-irradiated boron-doped silicon by combining density-functional modeling with the junction

03 February 2024 06:47:33



spectroscopy. A  $BI_2^+$  configuration with  $C_{2v}$  symmetry is identified as responsible for the carrier-induced formation of recombination centers corresponding to the previously characterized defect levels at 0.43 and 0.53 eV above  $E_v$ . Consistent with both experiments and calculations, its formation process is due to trapping by boron of two mono-interstitials with a migration barrier reduced to 0.5 eV when the immobile  $I^{2+}$  captures a photogenerated or injected electron. The diffusion barrier for  $BI_2^+$  is calculated to be 1.18 eV, and hence, the mobility of  $BI_2$  should be considered in situations such as TED.

## SUPPLEMENTARY MATERIAL

See the supplementary material for calculation details.

## ACKNOWLEDGMENTS

This work was supported by the NSF of China (Grant Nos. 12275247 and 12305341) and the Foundation of Science and Technology on Plasma Physics Laboratory (Grant No. 6142A04210105).

## AUTHOR DECLARATIONS

### Conflict of Interest

The authors have no conflicts to disclose.

### Author Contributions

**X. C. Chen:** Conceptualization (lead); Data curation (equal); Formal analysis (lead); Investigation (lead); Methodology (lead); Resources (lead); Software (equal); Validation (equal); Visualization (equal); Writing – original draft (lead); Writing – review & editing (lead). **L. Li:** Conceptualization (equal); Data curation (equal); Formal analysis (equal); Funding acquisition (lead); Investigation (equal); Methodology (equal); Project administration (lead); Validation (equal). **M. Y. Wang:** Data curation (lead); Formal analysis (equal); Investigation (equal); Validation (equal); Visualization (equal). **H. Ren:** Investigation (equal); Methodology (equal); Software (lead); Validation (equal). **X. Q. Liu:** Resources (equal); Validation (equal); Visualization (equal). **G. Zeng:** Formal analysis (equal); Writing – original draft (equal). **G. X. Yang:** Funding acquisition (equal).

## DATA AVAILABILITY

The data that support the findings of this study are available from the corresponding author upon reasonable request.

## REFERENCES

- <sup>1</sup>A. R. Meyer, P. C. Taylor, M. B. Venuti, S. Eley, V. LaSalvia, W. Nemeth, M. R. Page, D. L. Young, P. Stradins, and S. Agarwal, “Atomic structure of light-induced efficiency-degrading defects in boron-doped Czochralski silicon solar cells,” *Energy Environ. Sci.* **14**, 5416–5422 (2021).
- <sup>2</sup>I. Pintilie, E. Fretwurst, and G. Lindström, “Cluster related hole traps with enhanced-field-emission—The source for long term annealing in hadron irradiated Si diodes,” *Appl. Phys. Lett.* **92**, 024101 (2008).
- <sup>3</sup>R. Radu, I. Pintilie, L. C. Nistor, E. Fretwurst, G. Lindstroem, and L. F. Makarenko, “Investigation of point and extended defects in electron

irradiated silicon—Dependence on the particle energy,” *J. Appl. Phys.* **117**, 164503 (2015).

<sup>4</sup>L. F. Makarenko, S. B. Lastovskii, H. S. Yakushevich, M. Moll, and I. Pintilie, “Effect of electron injection on defect reactions in irradiated silicon containing boron, carbon, and oxygen,” *J. Appl. Phys.* **123**, 161576 (2018).

<sup>5</sup>R. Radu, I. Pintilie, L. F. Makarenko, E. Fretwurst, and G. Lindstroem, “Kinetics of cluster-related defects in silicon sensors irradiated with monoenergetic electrons,” *J. Appl. Phys.* **123**, 161402 (2018).

<sup>6</sup>R. M. Fleming, C. H. Seager, D. V. Lang, E. Bielejec, and J. M. Campbell, “Defect-driven gain bistability in neutron damaged, silicon bipolar transistors,” *Appl. Phys. Lett.* **90**, 172105 (2007).

<sup>7</sup>R. M. Fleming, C. H. Seager, D. V. Lang, and J. M. Campbell, “Transformation kinetics of an intrinsic bistable defect in damaged silicon,” *J. Appl. Phys.* **111**, 023715 (2012).

<sup>8</sup>X. Chen, L. Li, J. Zhang, Y. Jian, G. Yang, X. Liu, G. Zeng, Y. Pang, X. Yu, X. Meng, J. Shi, and X. Wu, “Metastable acceptors in boron doped silicon: Evidence of the defects contributing to carrier induced degradation,” *J. Phys. D: Appl. Phys.* **54**, 265103 (2021).

<sup>9</sup>S. B. Lastovskii, V. P. Markevich, H. S. Yakushevich, L. I. Murin, and V. P. Krylov, “Radiation-induced bistable centers with deep levels in silicon  $n^+-p$  structures,” *Semiconductors* **50**, 751–755 (2016).

<sup>10</sup>L. F. Makarenko, S. B. Lastovski, H. S. Yakushevich, E. Gaubas, J. Pavlov, V. V. Kozlovski, M. Moll, and I. Pintilie, “Formation of a bistable interstitial complex in irradiated  $p$ -type silicon,” *Phys. Status Solidi A* **216**, 1900354 (2019).

<sup>11</sup>V. E. Gusakov, S. B. Lastovskii, L. I. Murin, E. A. Tolkacheva, L. I. Khirunenko, M. G. Sosnin, A. V. Duvanskii, V. P. Markevich, M. P. Halsall, A. R. Peaker, I. Kolevator, H. M. Ayedh, E. V. Monakhov, and B. G. Svensson, “The di-interstitial in silicon: Electronic properties and interactions with oxygen and carbon impurity atoms,” *Phys. Status Solidi A* **214**, 1700261 (2017).

<sup>12</sup>L. Pelaz, M. Jaraiz, G. H. Gilmer, H. J. Gossmann, C. S. Rafferty, D. J. Eaglesham, and J. M. Poate, “B diffusion and clustering in ion implanted Si: The role of B cluster precursors,” *Appl. Phys. Lett.* **70**, 2285–2287 (1997).

<sup>13</sup>L. Pelaz, G. Gilmer, H. J. Gossmann, C. S. Rafferty, M. Jaraiz, and J. Barbolla, “B cluster formation and dissolution in Si: A scenario based on atomistic modeling,” *Appl. Phys. Lett.* **74**, 3657–3659 (1999).

<sup>14</sup>S. Chakravarthi and S. T. Dunham, “A simple continuum model for boron clustering based on atomistic calculations,” *J. Appl. Phys.* **89**, 3650–3655 (2001).

<sup>15</sup>M. Cogoni, A. Mattoni, B. P. Uberuaga, A. F. Voter, and L. Colombo, “Atomistic study of the dissolution of small boron interstitial clusters in c-Si,” *Appl. Phys. Lett.* **87**, 191912 (2005).

<sup>16</sup>P. López, M. Aboy, I. Munoz, I. Santos, L. A. Marqués, P. Fernández-Martínez, M. Ullán, and L. Pelaz, “Atomistic simulations of acceptor removal in  $p$ -type Si irradiated with neutrons,” *Nucl. Instrum. Methods Phys. Res. B* **512**, 42–48 (2022).

<sup>17</sup>P. López, M. Aboy, I. Santos, L. Marqués, M. Ullán, and L. Pelaz, “Microscopic origin of the acceptor removal in neutron-irradiated Si detectors—An atomistic simulation study,” *Acta Mater.* **241**, 118375 (2022).

<sup>18</sup>M. D. Segall, P. J. D. Lindan, M. J. Probert, C. J. Pickard, P. J. Hasnip, S. J. Clark, and M. C. Payne, “First-principles simulation: Ideas, illustrations and the CASTEP code,” *J. Phys.: Condens. Matter* **14**, 2717 (2002).

<sup>19</sup>D. Vanderbilt, “Soft self-consistent pseudopotentials in a generalized eigenvalue formalism,” *Phys. Rev. B* **41**, 7892–7895 (1990).

<sup>20</sup>J. P. Perdew, K. Burke, and M. Ernzerhof, “Generalized gradient approximation made simple,” *Phys. Rev. Lett.* **77**, 3865 (1996).

<sup>21</sup>J. Heyd, G. E. Scuseria, and M. Ernzerhof, “Hybrid functionals based on a screened Coulomb potential,” *J. Chem. Phys.* **118**, 8207–8215 (2003).

<sup>22</sup>A. V. Krukau, O. A. Vydrov, A. F. Izmaylov, and G. E. Scuseria, “Influence of the exchange screening parameter on the performance of screened hybrid functionals,” *J. Chem. Phys.* **125**, 224106 (2006).

<sup>23</sup>M. E. Batten, J. Coutinho, H. M. Ayedh, J. Ul Hassan, I. Farkas, S. Öberg, Y. K. Frodason, B. G. Svensson, and L. Vines, “Anisotropic and plane-selective migration of the carbon vacancy in SiC: Theory and experiment,” *Phys. Rev. B* **100**, 014103 (2019).

- <sup>24</sup>H. M. Ayedh, E. V. Monakhov, and J. Coutinho, "Formation and dissociation reactions of complexes involving interstitial carbon and oxygen defects in silicon," *Phys. Rev. Mater.* **4**, 064601 (2020).
- <sup>25</sup>G. Henkelman and H. Jónsson, "Improved tangent estimate in the nudged elastic band method for finding minimum energy paths and saddle points," *J. Chem. Phys.* **113**, 9978–9985 (2000).
- <sup>26</sup>C. Freysoldt, B. Grabowski, T. Hickel, J. Neugebauer, G. Kresse, A. Janotti, and C. G. Van de Walle, "First-principles calculations for point defects in solids," *Rev. Mod. Phys.* **86**, 253 (2014).
- <sup>27</sup>H. P. Komsa, T. T. Rantala, and A. Pasquarello, "Finite-size supercell correction schemes for charged defect calculations," *Phys. Rev. B* **86**, 045112 (2012).
- <sup>28</sup>A. Resende, R. Jones, S. Öberg, and P. R. Briddon, "Calculations of electrical levels of deep centers: Application to Au-h and Ag-h defects in silicon," *Phys. Rev. Lett.* **82**, 2111 (1999).
- <sup>29</sup>M. Goss, J. Shaw, and P. Briddon, "Marker-method calculations for electrical levels using Gaussian-orbital basis sets," in *Theory of Defects in Semiconductors* (Springer, Berlin, 2007), pp. 69–94. doi:10.1007/11690320\_4.
- <sup>30</sup>C. Freysoldt, J. Neugebauer, and C. G. Van de Walle, "Fully ab initio finite-size corrections for charged-defect supercell calculations," *Phys. Rev. Lett.* **102**, 016402 (2009).
- <sup>31</sup>A. Carvalho and A. H. Castro Neto, "Donor and acceptor levels in semiconducting transition-metal dichalcogenides," *Phys. Rev. B* **89**, 081406(R) (2014).
- <sup>32</sup>A. R. Peaker, V. P. Markevich, and J. Coutinho, "Tutorial: Junction spectroscopy techniques and deep-level defects in semiconductors," *J. Appl. Phys.* **123**, 161559 (2018).
- <sup>33</sup>H.-P. Komsa and A. Pasquarello, "Finite-size supercell correction for charged defects at surfaces and interfaces," *Phys. Rev. Lett.* **110**, 095505 (2013).
- <sup>34</sup>T. M. Vincent, S. K. Estreicher, J. Weber, V. Kolkovsky, and N. Yarykin, "The Cu photoluminescence defect and the early stages of Cu precipitation in Si," *J. Appl. Phys.* **127**, 085704 (2020).
- <sup>35</sup>A. Carvalho, R. Jones, M. Sanati, S. K. Estreicher, J. Coutinho, and P. R. Briddon, "First-principles investigation of a bistable boron-oxygen interstitial pair in Si," *Phys. Rev. B* **73**, 245210 (2006).
- <sup>36</sup>J. Coutinho, V. P. Markevich, A. R. Peaker, B. Hamilton, S. B. Lastovskii, L. I. Murin, B. J. Svensson, M. J. Rayson, and P. R. Briddon, "Electronic and dynamical properties of the silicon trivacancy," *Phys. Rev. B* **86**, 174101 (2012).
- <sup>37</sup>J. Lindroos, D. P. Fenning, D. J. Backlund, E. Verlage, A. Gorgulla, S. K. Estreicher, H. Savin, and T. Buonassisi, "Nickel: A very fast diffuser in silicon," *J. Appl. Phys.* **113**, 204906 (2013).
- <sup>38</sup>V. P. Markevich, S. Leonard, A. R. Peaker, B. Hamilton, A. G. Marinopoulos, and J. Coutinho, "Titanium in silicon: Lattice positions and electronic properties," *Appl. Phys. Lett.* **104**, 152105 (2014).
- <sup>39</sup>E. Wright, J. Coutinho, S. Öberg, and V. J. B. Torres, "Mössbauer parameters of Fe-related defects in group-IV semiconductors: First principles calculations," *J. Appl. Phys.* **119**, 023715 (2012) (2016).
- <sup>40</sup>D. J. Backlund, T. M. Gibbons, and S. K. Estreicher, "Vanadium interactions in crystalline silicon," *Phys. Rev. B* **94**, 195210 (2016).
- <sup>41</sup>T. M. Gibbons, D. J. Backlund, and S. K. Estreicher, "Cobalt-related defects in silicon," *J. Appl. Phys.* **121**, 045704 (2017).
- <sup>42</sup>T. M. Vincent and S. K. Estreicher, "Ag and Ag–Cu interactions in Si," *J. Appl. Phys.* **128**, 155703 (2020).
- <sup>43</sup>J. Coutinho, D. Gomes, V. J. B. Torres, T. O. A. Fattah, V. P. Markevich, and A. R. Peaker, "Theory of reactions between hydrogen and group-III acceptors in silicon," *Phys. Rev. B* **108**, 014111 (2023).
- <sup>44</sup>L. Yang, R. Fan, A. Hu, J. Ma, Y. Liu, and Y. Lu, "Tuning donor level of nitrogen-doped diamond by deep strain engineering—An ab initio study," *Appl. Phys. Lett.* **123**, 062105 (2023).
- <sup>45</sup>L. Seixas, A. Carvalho, and A. H. Castro Neto, "Atomically thin dilute magnetism in Co-doped phosphorene," *Phys. Rev. B* **91**, 155138 (2015).
- <sup>46</sup>L. C. Gomes, A. Carvalho, and A. H. Castro Neto, "Vacancies and oxidation of two-dimensional group-IV monochalcogenides," *Phys. Rev. B* **94**, 054103 (2016).
- <sup>47</sup>K. J. Xiao, A. Carvalho, and A. H. Castro Neto, "Defects and oxidation resilience in InSe," *Phys. Rev. B* **96**, 054112 (2017).
- <sup>48</sup>L. Li, J. M. Shi, X. Q. Liu, J. Q. Yang, X. W. Wang, Z. H. Li, P. Zheng, and G. Zeng, "Current gain degradation model of displacement damage for drift BJTs," *IEEE Trans. Nucl. Sci.* **66**, 716–723 (2019).
- <sup>49</sup>L. Li, X. C. Chen, Y. Jian, Z. H. Li, Y. Z. Wu, J. P. Zhang, M. Ren, B. Zhang, X. L. Wu, Y. L. Pang, and G. X. Yang, "Improved model for ionization-induced surface recombination current in *pnp* BJTs," *IEEE Trans. Nucl. Sci.* **67**, 1826–1834 (2020).
- <sup>50</sup>J. Kim, F. Kirchhoff, W. G. Aulbur, J. W. Wilkins, F. S. Khan, and G. Kresse, "Thermally activated reorientation of di-interstitial defects in silicon," *Phys. Rev. Lett.* **83**, 1990 (1999).
- <sup>51</sup>D. A. Richie, J. Kim, S. A. Barr, K. R. A. Hazzard, R. Hennig, and J. W. Wilkins, "Complexity of small silicon self-interstitial defects," *Phys. Rev. Lett.* **92**, 045501 (2004).
- <sup>52</sup>G. M. Lopez and V. Fiorentini, "Structure, energetics, and extrinsic levels of small self-interstitial clusters in silicon," *Phys. Rev. B* **69**, 155206 (2004).
- <sup>53</sup>X. Y. Liu, W. Windl, and M. P. Masquelier, "Ab initio modeling of boron clustering in silicon," *Appl. Phys. Lett.* **77**, 2018–2020 (2000).
- <sup>54</sup>G. S. Hwang and W. A. Goddard, "Catalytic role of boron atoms in self-interstitial clustering in Si," *Appl. Phys. Lett.* **83**, 1047–1049 (2003).
- <sup>55</sup>P. Deák, A. Gali, A. Sólyom, P. Ordejón, K. Kamarás, and G. Battistig, "Studies of boron-interstitial clusters in Si," *J. Phys.: Condens. Matter* **15**, 4967 (2003).
- <sup>56</sup>X. Y. Liu and W. Windl, "Theoretical study of boron clustering in silicon," *J. Comput. Electron.* **4**, 203–219 (2005).
- <sup>57</sup>P. Deák, A. Gali, A. Sólyom, A. Buruzs, and T. Frauenheim, "Electronic structure of boron-interstitial clusters in silicon," *J. Phys.: Condens. Matter* **17**, S2141 (2005).
- <sup>58</sup>N. E. B. Cowern, G. Mannino, P. A. Stolk, F. Roozeboom, H. G. A. Huizing, J. G. M. van Berkum, F. Cristiano, A. Claverie, and M. Jaraiz, "Energetics of self-interstitial clusters in Si," *Phys. Rev. Lett.* **82**, 4460 (1999).
- <sup>59</sup>M. P. Chichkine and M. M. De Souza, "Dynamics of self-interstitial cluster formation in silicon," *Phys. Rev. B* **66**, 045205 (2002).
- <sup>60</sup>S. Lee and G. S. Hwang, "Structure and stability of small compact self-interstitial clusters in crystalline silicon," *Phys. Rev. B* **77**, 085210 (2008).
- <sup>61</sup>I. Martin-Bragado, M. Jaraiz, P. Castrillo, R. Pinacho, J. Barbolla, and M. M. De Souza, "Mobile silicon di-interstitial: Surface, self-interstitial clustering, and transient enhanced diffusion phenomena," *Phys. Rev. B* **68**, 195204 (2003).
- <sup>62</sup>S. M. Myers, P. J. Cooper, and W. R. Wampler, "Model of defect reactions and the influence of clustering in pulse-neutron-irradiated Si," *J. Appl. Phys.* **104**, 044507 (2008).
- <sup>63</sup>S. Ma and S. Wang, "Ab initio study of self-diffusion in silicon over a wide temperature range: Point defect states and migration mechanisms," *Phys. Rev. B* **81**, 193203 (2010).
- <sup>64</sup>J. A. Stewart, N. A. Modine, and R. Dingreville, "Re-examining the silicon self-interstitial charge states and defect levels: A density functional theory and bounds analysis study," *AIP Adv.* **10**, 095004 (2020).
- <sup>65</sup>P. Rinke, A. Janotti, M. Scheffler, and C. G. Van de Walle, "Defect formation energies without the band-gap problem: Combining density-functional theory and the gw approach for the silicon self-interstitial," *Phys. Rev. Lett.* **102**, 026402 (2009).
- <sup>66</sup>R. Jones, T. A. G. Eberlein, N. Pinho, B. J. Coomer, J. P. Goss, P. R. Briddon, and S. Öberg, "Self-interstitial clusters in silicon," *Nucl. Instrum. Methods Phys. Res. B* **186**, 10–18 (2002).
- <sup>67</sup>R. Jones, A. Carvalho, J. P. Goss, and P. R. Briddon, "The self-interstitial in silicon and germanium," *Mater. Sci. Eng. B* **159**, 112–116 (2009).
- <sup>68</sup>W. Gao and A. Tkatchenko, "Electronic structure and van der Waals interactions in the stability and mobility of point defects in semiconductors," *Phys. Rev. Lett.* **111**, 045501 (2013).
- <sup>69</sup>Y. A. Du, R. G. Hennig, and J. W. Wilkins, "Diffusion mechanisms for silicon di-interstitials," *Phys. Rev. B* **73**, 245203 (2006).

- <sup>70</sup>Y. Kim, T. A. Kirichenko, N. Kong, G. Henkelman, and S. K. Banerjee, "First-principles studies of small arsenic interstitial complexes in crystalline silicon," *Phys. Rev. B* **79**, 075201 (2009).
- <sup>71</sup>C. A. Londos, G. Antonaras, and A. Chroneos, "Di-interstitial defect in silicon revisited," *J. Appl. Phys.* **114**, 193513 (2013).
- <sup>72</sup>J. W. Jeong and A. Oshiyama, "Atomic and electronic structures of a boron impurity and its diffusion pathways in crystalline Si," *Phys. Rev. B* **64**, 235204 (2001).
- <sup>73</sup>J. Schmidt and K. Bothe, "Structure and transformation of the metastable boron-and oxygen-related defect center in crystalline silicon," *Phys. Rev. B* **69**, 024107 (2004).
- <sup>74</sup>D. W. Palmer, K. Bothe, and J. Schmidt, "Kinetics of the electronically stimulated formation of a boron-oxygen complex in crystalline silicon," *Phys. Rev. B* **76**, 035210 (2007).
- <sup>75</sup>J. Adey, R. Jones, D. W. Palmer, P. R. Briddon, and S. Öberg, "Degradation of boron-doped Czochralski-grown silicon solar cells," *Phys. Rev. Lett.* **93**, 055504 (2004).
- <sup>76</sup>M.-H. Du, H. M. Branz, R. S. Crandall, and S. B. Zhang, "Bistability-mediated carrier recombination at light-induced boron-oxygen complexes in silicon," *Phys. Rev. Lett.* **97**, 256602 (2006).
- <sup>77</sup>L. I. Murin, E. A. Tolkacheva, V. P. Markevich, A. R. Peaker, B. Hamilton, E. Monakhov, B. G. Svensson, J. L. Lindström, P. Santos, J. Coutinho, and A. Carvalho, "The oxygen dimer in Si: Its relationship to the light-induced degradation of Si solar cells?," *Appl. Phys. Lett.* **98**, 182101 (2011).
- <sup>78</sup>S. M. Kim, S. Chun, S. Bae, S. Park, M. G. Kang, H. E. Song, Y. Kang, H. S. Lee, and D. Kim, "Light-induced degradation and metastable-state recovery with reaction kinetics modeling in boron-doped Czochralski silicon solar cells," *Appl. Phys. Lett.* **105**, 083509 (2014).